First-principles study of point defects in rutile TiO_{2-x}

Eunae Cho and Seungwu Han*
Department of Physics and Division of Nano Science, Ewha Womans University, Seoul 120-750, Korea

Hyo-Shin Ahn and Kwang-Ryeol Lee
Future Technology Research Division, Korea Institute of Science and Technology, Seoul 136-791, Korea

Seong Keun Kim and Cheol Seong Hwang
School of Materials Science and Engineering and Inter-University Semiconductor Research Center, Seoul National University, Seoul, 151-742, Korea

(Received 4 August 2005; revised manuscript received 30 January 2006; published 9 May 2006)

We report our first-principles results on point defects in TiO_2 in the rutile phase. Both the oxygen vacancy and titanium interstitial are considered. The size effect of the supercell has been examined and the localized state associated with the oxygen vacancy turns out to be sensitive to the supercell size. We find that the oxygen vacancy does not give rise to a defect level within the energy gap while the titanium interstitial creates a localized state 0.2 eV below the conduction edge that can be related to the infrared absorption data. The charge accumulation around the oxygen vacancy is attributed to polarization of valence bands.

DOI: 10.1103/PhysRevB.73.193202 PACS number(s): 61.72.Ji, 71.15.Mb, 77.84.Dy, 68.55.Ln

Titanium dioxide (TiO_2) is a material of wide applications ranging from a substance for white pigment to photocatalysts and nanoscale electronic devices. There are two important phases of TiO_2, anatase and rutile. While the surface of the anatase phase is well known for efficient photocatalytic effects, the high dielectric constants of the rutile phase ($\varepsilon = 30-80$) have made it a candidate material as a nanoscale insulator such as an ultrathin gate oxide in field-effect transistors[1,2] or a dielectric layer in capacitors for dynamic random access memory.[3]

Under the usual growth conditions, an oxygen-deficient phase of rutile TiO_{2-x} is found with x typically less than 0.008. For larger values of x, the phase diagram of TiO_2 indicates that the Magneli phase is more stable.[4] To explain the conductivity behavior of the reduced rutile with respect to varying temperatures and oxygen partial pressures, defect models considering three types of point defects were proposed; a Ti^{3+} interstitial, a Ti^{4+} interstitial, and a doubly ionized oxygen vacancy.[5] Tracer-diffusion experiments favor an interstitial mechanism of Ti diffusion. The electronic and optical properties of the nonstochiometric oxides critically depend on defect structures existing within the material. For example, leakage currents in the TiO_2 insulator are often explained on the basis of gap states originating from various point defects.[1] Another example is that oxygen vacancies at the TiO_2 surface influence the adsorption of molecules.[6] Therefore, the study of the electronic structure in the presence of point defects is very important to understand the material properties of oxides. While there have been many theoretical investigations of point defects in TiO_2 surface,[7,8] relatively few attempts have been made to investigate the electronic structures associated with point defects in the bulk phase.[9–11] The empirical nature of the methods used in the literature[9,11] necessitates a first-principles investigation of point defects in TiO_2, which will serve as a firm basis to understand defect-related phenomena. In this paper, we carry out first-principles calculations to study the oxygen vacancy and titanium interstitial, two elemental point defects in TiO_{2-x}. We carefully examine atomic relaxations around the point defects and related features in the electronic structure.

The density functional calculations are performed using a computational code, the Vienna *ab initio* simulation package (VASP).[12] To check any effect of different implementation of first-principles method, some results are repeated using another code based on similar methods.[13] We employ a plane-wave basis set with an energy cutoff of 400 eV to describe the electronic wave function. The ionic potentials are described by projector augmented-wave pseudopotentials[14] and the exchange-correlation energy of the electrons is approximated by a local density functional presented in Ref. 15. $3d$ and $4s$ ($2s$ and $2p$) states are treated as valence electrons for Ti (O) atoms. For the k-point integration, we use a $4\times4\times6$ mesh for the primitive cell (shown in Fig. 1) and the Γ point for $3\times3\times5$ supercells. The atomic positions are relaxed until the Hellmann-Feynman force on each atom is reduced to within 0.01 eV/Å. To obtain the equilibrium lattice parameters and bulk modulus of the crystalline phase, we additionally relax the cell shape and volume to match with external pressures.

Figure 1 shows the unit cell of TiO_2 in the rutile phase. Computational results for structural parameters are summarized in Table I. The structural parameters agree well with

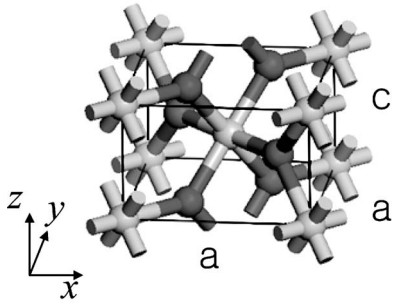

FIG. 1. Tetragonal unit cell of rutile TiO_2. The relative ionic positions are (0,0,0) and (1/2,1/2,1/2) for Ti atoms, and $(u,u,0)$, $(1-u,1-u,0)$, $(1/2+u,1/2-u,1/2)$, and $(1/2-u,1/2+u,1/2)$ for O atoms.

TABLE I. Structural parameters, bulk modulus, and energy gap (E_{gap}) of TiO_2 in comparison with experimental data and other theoretical results. Theoretical value of direct band gap is measured at Γ point.

	a (Å)	c (Å)	u	B (GPa)	E_{gap} (eV)
Experiment[a]	4.587	2.954	0.305	216	3.0
This work	4.536	2.914	0.304	265	1.7
Theory[b]	4.653	2.965	0.305	240	2.0
Theory[c]	4.536	2.915	0.304	N/A	1.87

[a]Burdett *et al.* (Ref. 16).
[b]Glassford *et al.* (Ref. 17).
[c]Lee *et al.* (Ref. 18).

the experimental values within 2%. The underestimation of the energy gap is due to the local density approximation. From the analysis of the partial density of states, we find that the conduction bands are mostly Ti 3*d* states while the valence bands have mainly O 2*p* character, confirming that TiO_2 is a charge-transfer insulator.

Due to the periodic boundary condition imposed by the plane-wave basis, defects are repeated in a crystalline structure. It is an important step to confirm whether the computational results are affected by the supercell dimension. In previous first-principles work, 48 atoms in eight unit cells ($2\times2\times2$ supercell) were typical sizes adopted for studying defect properties in bulk rutile.[7,8] The shortest defect-defect distances in these supercells are ~6 Å which may not be enough to neglect the interaction between defects. To investigate the size effect, we compare in Fig. 2 the band structures of a supercell with and without one oxygen vacancy in $2\times2\times2$ and $3\times3\times5$ supercells. The $3\times3\times5$ supercell is the largest supercell we could try within our computational resources. The band structures around the Fermi level are shown since defect states in this range will influence the electronic and optical properties of TiO_2 substantially. The relatively flat band in Fig. 2(b) (see the arrow) corresponds to the localized defect states with the energy level close to the conduction band edge. This state has most of its weight in three Ti atoms surrounding the oxygen vacancy. On the other hand, for a larger $3\times3\times5$ supercell containing 90 cations and 180 (or 179) anions [Figs. 2(c) and 2(d)], the defect level indicated by an arrow is found to shift up substantially and be almost unoccupied. This indicates that positive charges at the vacancy site are not strong enough to hold electrons locally or create an *F* center within the band gap. This is in part due to the ionic displacements (see below), especially those of nearby Ti atoms. In fact, when atoms are fixed at the bulk position, we find that the oxygen vacancy creates a defect state within the energy gap. The outward relaxation of Ti atoms effectively screens the positive charge of the oxygen vacancy. The shift of localized defect levels with increasing supercell size is similar to the case of an oxygen vacancy in $SrTiO_3$ as recently reported.[19,20] The dispersion in the defect state for the $3\times3\times5$ supercell indicates that one still needs a larger supercell to accurately characterize the localized level. However, the qualitative nature of the defect state, such as the relative position from the conduction minimum, is well addressed in the $3\times3\times5$ supercell. Therefore, we use larger $3\times3\times5$ supercells throughout the rest of the calculation for point defects, to make sure that the computed defect properties are free from the supercell size effect as much as possible.

We first study an oxygen vacancy in rutile TiO_2, which is the most important point defect in the reduced TiO_2 sample. It is well known that ionized oxygen vacancies effectively dope TiO_2 with electrons, resulting in a *n*-type transport behavior. In our calculations, the oxygen vacancy is created simply by taking out one oxygen atom from the supercell. After relaxation, the total energy is lowered by 1.69 eV from the initial energy and surrounding Ti atoms are displaced by 0.27–0.30 Å outward from the vacancy site. This is due to the effectively positive charges of the vacancy site which

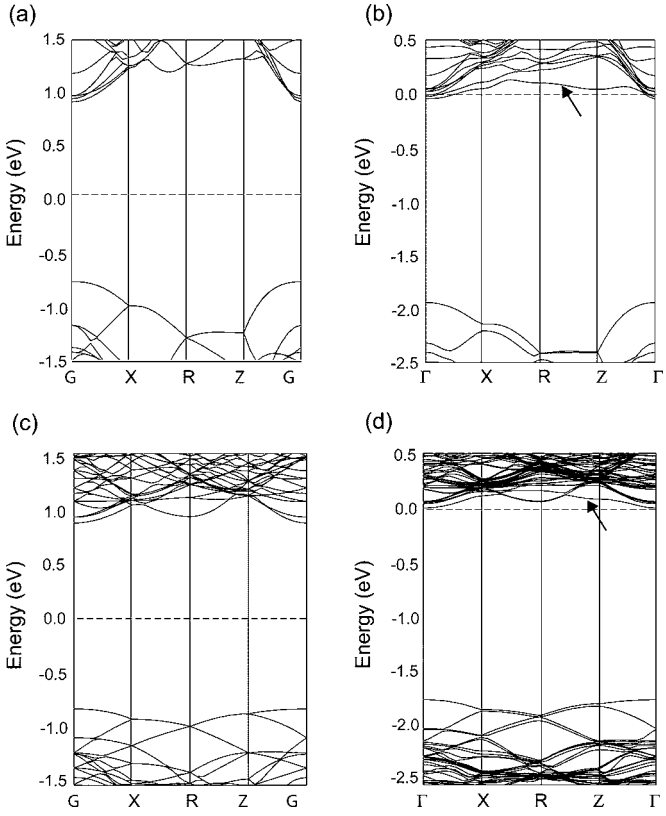

FIG. 2. Comparison of band structures of TiO_2 supercells with or without single oxygen vacancy. (a) is for perfect $2\times2\times2$ supercell and (b) is for the same supercell including one oxygen vacancy. (c) and (d) are similar to (a) and (b) except that they are results for $3\times3\times5$ supercells. The Fermi levels, indicated by dashed lines, are set to zero.

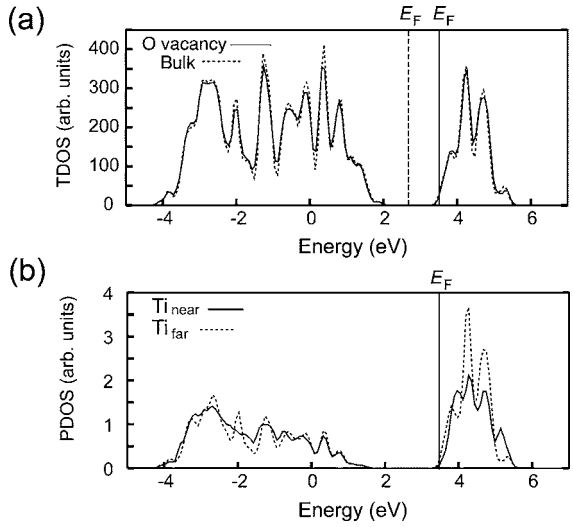

FIG. 3. (a) Total density of states for TiO_2 with the oxygen vacancy compared with that of the perfect crystal. The Fermi levels (E_F) are shown as vertical lines. (b) Partial density of states for the supercell containing the oxygen vacancy. Ti_{near} indicates one of three Ti atoms neighboring the vacancy site and Ti_{far} is the Ti atom furthest from the vacancy site.

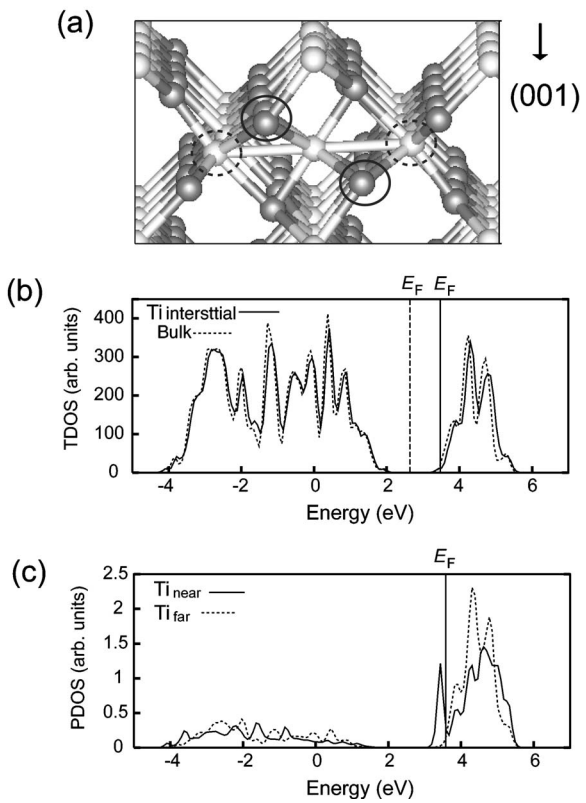

FIG. 4. (a) The relaxed geometry around the Ti interstitial. Dark and light grayspheres indicate O and Ti atoms, respectively. The atoms within circles are under largest relaxations. (b) Total density of states of TiO_2 with the Ti interstitial. (c) Partial density of states for the interstitial Ti atom (Ti_{int}) and the Ti atom furthest from the interstitial site.

interact repulsively with nearby cations. We calculate the electronic population at each atomic site by integrating the total electronic charges inside a sphere centered on each atom with effective ionic radii, the so-called Shannon-Prewitt radii.[21] They are 0.61 and 1.36 Å for Ti and O atoms, respectively. We find that the electron population of three Ti atoms surrounding the oxygen vacancy substantially increases from the bulk value of $0.968e$ to $1.021e$ while those at other Ti atoms change less than $0.02e$, consistent with the positive character of the vacancy charge.

In Fig. 3(a), the total density of states (TDOS) is compared between supercells with and without the oxygen vacancy. The Fermi level is just above the conduction band, leading to *n*-type doping of TiO_2. As can be seen in Fig. 2(d), the dispersion of occupied states in the conduction bands indicates that they are distributed over the whole supercell. This raises a question whether extra electrons occupying Ti atoms near the vacancy site originate from the conduction band or not. The analysis of the occupied states in the conduction band indicates that they are uniformly distributed with Ti *d* character. In other words, the additional electrons at nearby Ti atoms are contributed by valence states. To confirm this, we carry out a calculation with two fewer electrons. This shifts down the Fermi level to be within the original band gap. However, the charge accumulation at Ti atoms around the vacancy is almost unchanged, indicating that extra electrons mainly originate from the small polarization of the valence states.

Figure 3(b) shows the partial density of states (PDOS) of one of three nearby Ti atoms in comparison with that of a Ti atom furthest from the vacancy site. It can be seen that the two PDOS curves behave in a similar way near the Fermi level. To investigate whether vacancy clustering leads to creation of localized gap states, we also calculate divacancies by removing two oxygen atoms from $3\times3\times5$ supercells in nearest-neighbor or apical positions around a specific Ti atom. The internal coordinates of all atoms within the supercells are fully relaxed. We identify an in-gap state only for an apical divacancy. The defect level is located about 0.2 eV below the conduction minimum. The spatial distribution of this localized state shows a *d* character at the Ti site between two oxygen vacancies. However, the total energy of the apical divacancy is higher by 0.58 eV compared to the nearest-neighbor divacancy, indicating that the apical one is rather unstable.

Next we calculate a Ti interstitial, another possible point defect in nonstoichiometric TiO_{2-x}. The initial position of an interstitial Ti atom is chosen to be the empty octahedral site, i.e., the center of the (010) face [or equivalently the (100) face] in Fig. 1. In Fig. 4(a), an interstitial Ti atom and the nearby atoms are shown at relaxed positions. We also change the starting position of the interstitial Ti atoms along the *z* axis and confirm that octahedral sites are the most stable position of Ti interstitials. Due to the open structure of the rutile phase along the [001] direction, relatively small relaxations are found around the Ti interstitial compared to the case of the oxygen vacancy. As can be seen in Fig. 4(a), the closest Ti atoms (dashed circles) relax outward from the interstitial site by 0.26 Å while the nearest four O atoms (solid circles) are pulled in toward the cation interstitial by 0.21 Å. The partial charges inside ionic radii are $1.103e$ for the Ti

interstitial and $(1.00-1.04)e$ for six neighboring Ti atoms. (The bulk value is $0.968e$.) These values are similar to the case of the oxygen vacancy. The relatively large effective charge of the Ti interstitial is related to the localized level. (See below.)

The TDOS in the presence of Ti interstitial is shown in Fig. 4(b). Two electrons are occupying the conduction bands that are certainly donated by the Ti interstitial. Figure 4(c) shows the PDOS around the Ti interstitial. One can find that the PDOS of the interstitial Ti atom is quite different from those of the other Ti atoms, with a pronounced peak appearing just below the Fermi level. This is a localized state around the Ti interstitial with the energy level approximately 0.2 eV below the conduction minimum of TiO_2. Inspection of the wave function of this in-gap state shows that the orbital character is mainly the $3d(x^2-y^2)$ orbital of the Ti interstitial slightly mixed with the $3d(3z^2-r^2)$ component. To confirm the localized nature of this band-gap state, we calculate the band dispersion along Γ to Z and Γ to X. The bandwidth of the localized state is less than 0.02 eV while those of extended Ti $3d$ states are always bigger than 0.1 eV. The occupation of the localized level at the Ti interstitial indicates that only two electrons are transferred to conduction bands as free carriers, a number that can increase with the temperature.

To determine the relative stability between point defects, we compare defect formation energies (E_{for}) of two point defects using the following formula:

$$E_{\text{for}} = E_{\text{tot}}(\text{defect}) - n_{\text{Ti}}\mu_{\text{Ti}} - n_{\text{O}}\mu_{\text{O}}, \quad (1)$$

where E_{tot}(defect) is the total energy of the supercell containing a defect. n_i and μ_i are the number and chemical potential of the constituent atoms, respectively, satisfying the relation $\mu_{\text{Ti}}+2\mu_{\text{O}}=E_{\text{tot}}(\text{bulk})/2$. Assuming μ_{O} is half the total energy of an oxygen molecule, the formation energies are 7.09 and 4.44 eV for the Ti interstitial and oxygen vacancy, respectively, indicating that formation of the oxygen vacancy is energetically favored. However, the relative stability is reversed at $\mu_{\text{O}}=E_{\text{tot}}(O_2)/2-2.64$ eV, corresponding to a Ti-richer environment, where the formation energies of the two defects are equally 1.8 eV. It is noted that the defect level for the Ti interstitial is of a localized d character and unphysical self-interactions of occupied electrons may influence the formation energy of the Ti interstitial unfavorably. We also add that our calculations are for neutral defects in the sense that charge neutrality is maintained without uniform background charges. However, the delocalized characters of doped electrons imply that charge states of point defects are more consistent with +2 for both the oxygen vacancy and Ti interstitial. The Ti^{2+} interstitial found in our calculation is rather at variance with the traditional picture of this defect, i.e., Ti^{4+} or Ti^{3+}. There are several possible causes for the discrepancy, such as the defect clustering or the accuracy of the local density approximation (LDA).

The transition from this localized state to the conduction band may account for an absorption peak around 0.75 eV found in the literature.[22] The discrepancy of 0.55 eV could be attributed to the localized nature of d electrons, which could be addressed by the LDA+U formalism.[23] In passing, it is worthwhile to mention that spin density functional calculations for the oxygen vacancy and Ti interstitial are performed as well but the spin moments are close to zero. Therefore, the computational results are essentially the same as those in spin-paired calculations. This is because the electronic states are either delocalized or, if localized, doubly occupied.

In summary, we perform first-principles density functional calculations on the oxygen vacancy and Ti interstitial in rutile TiO_2. The defect level associated with the oxygen vacancy is not identified within the energy gap while the Ti interstitial gives rise to a defect level that can be related to the infrared experiment.

This work was supported by the System IC2010 program of the Korean government, the National Program for 0.1 Terabit NVM Devices, and by the KOSEF through CSCMR and National Research Laboratory (NRL) program. The computations were carried out at KISTI through Sixth Strategic Supercomputing Program.

*Corresponding author. Electronic address: hansw@ewha.ac.kr

[1] S. A. Campbell *et al.*, IBM J. Res. Dev. **43**, 383 (1999).
[2] C. K. Maiti *et al.*, Microelectron. Eng. **72**, 253 (2004).
[3] S. K. Kim *et al.*, Appl. Phys. Lett. **85**, 4112 (2004).
[4] J. S. Anderson and A. S. Khan, J. Less-Common Met. **22**, 219 (1970).
[5] K. Hoshino, N. L. Peterson, and C. L. Wiley, J. Phys. Chem. Solids **46**, 1397 (1985).
[6] X. Wu *et al.*, Phys. Rev. B **68**, 241402(R) (2003).
[7] M. Ramamoorthy, R. D. King-Smith, and D. Vanderbilt, Phys. Rev. B **49**, 7709 (1994), and references therein.
[8] P. J. D. Lindan, N. M. Harrison, M. J. Gillan, and J. A. White, Phys. Rev. B **55**, 15919 (1997), and references therein.
[9] A. Stashans, S. Lunell, and R. W. Grimes, J. Phys. Chem. Solids **57**, 1293 (1996).
[10] J. He and S. B. Sinnott, J. Am. Ceram. Soc. **88**, 737 (2005).
[11] N. Yu and J. W. Halley, Phys. Rev. B **51**, 4768 (1995).
[12] G. Kresse and J. Hafner, Phys. Rev. B **47**, 558(R) (1993); **49**, 14251 (1994).
[13] S. Baroni, A. Dal Corso, S. de Gironcoli, and P. Giannozzi, http://www.pwscf.org
[14] P. E. Blöchl, Phys. Rev. B **50**, 17953 (1994).
[15] J. P. Perdew and A. Zunger, Phys. Rev. B **23**, 5048 (1981).
[16] J. K. Burdett *et al.*, J. Am. Chem. Soc. **109**, 3639 (1987).
[17] K. M. Glassford and J. R. Chelikowsky, Phys. Rev. B **46**, 1284 (1992).
[18] C. Lee, P. Ghosez, and X. Gonze, Phys. Rev. B **50**, 13379 (1994).
[19] J. P. Buban, H. Iddir, and S. Ogut, Phys. Rev. B **69**, 180102(R) (2004).
[20] W. Luo, W. Duan, S. G. Louie, and M. L. Cohen, Phys. Rev. B **70**, 214109 (2004).
[21] R. D. Shannon and C. T. Prewitt, Acta Crystallogr., Sect. B: Struct. Crystallogr. Cryst. Chem. **25**, 925 (1969).
[22] D. C. Cronemeyer, Phys. Rev. **113**, 1222 (1959).
[23] E. Pavarini *et al.*, Phys. Rev. Lett. **92**, 176403 (2004).